Published OnlineFirst April 28, 2020; DOI: 10.1158/1078-0432.CCR-19-3925

Tumor CD155 Expression Is Associated with Resistance to Anti-PD1 Immunotherapy in Metastatic Melanoma

Ailin Lepletier[1], Jason Madore[1], Jake S. O'Donnell[1,2,3], Rebecca L. Johnston[4], Xian-Yang Li[1], Elizabeth McDonald[2], Elizabeth Ahern[1,3,5], Anna Kuchel[1,3,5], Melissa Eastgate[3,5], Sally-Ann Pearson[1], Domenico Mallardo[6], Paolo A. Ascierto[6], Daniela Massi[7], Barbara Merelli[8], Mario Mandala[8], James S. Wilmott[9], Alexander M. Menzies[9], Charles Leduc[10], John Stagg[1,11], Bertrand Routy[11], Georgina V. Long[9], Richard A. Scolyer[9,12,13], Tobias Bald[14], Nicola Waddell[4], William C. Dougall[1], Michele W. L. Teng[2,3], and Mark J. Smyth[1,3]

ABSTRACT

Purpose: Resistance to anti-PD1–based immune checkpoint blockade (ICB) remains a problem for the treatment of metastatic melanoma. Tumor cells as well as host myeloid cells can express the immune checkpoint ligand CD155 to regulate immune cell function. However, the effect of tumor CD155 on the immune context of human melanoma has not been well described. This observational study characterizes tumor CD155 ligand expression by metastatic melanoma tumors and correlates results with differences in immune cell features and response to ICB.

Experimental Design: Pretreatment tumor specimens, from 155 patients with metastatic melanoma treated with ICB and from 50 patients treated with BRAF/MEK-directed targeted therapy, were assessed for CD155 expression by IHC. Intratumor T-cell features were analyzed using multiplex-immunohistofluorescence for CD8, PD1, and SOX10. Correlations were made between CD155 tumor level and bulk tumor RNA sequencing results, as well as clinical RECIST response and progression-free survival.

Results: High pretreatment CD155 tumor levels correlated with high parenchymal $PD1^+CD8^+/CD8^+$ T-cell ratios ($PD1^{tR}$) and poor response to anti-PD1 therapy. In PDL1 negative tumors, high CD155 tumor expression was associated with patients who had poor response to combination anti-PD1/CTLA4 therapy.

Conclusions: Our findings are the first to suggest that tumor CD155 supports an increase in the fraction of $PD1^+CD8^+$ T cells in anti-PD1 refractory melanoma tumors and, further, that targeting the CD155 pathway might improve response to anti-PD1 therapy for patients with metastatic melanoma.

Introduction

Tumor cells can upregulate immune checkpoint ligands to suppress T-cell function (1–3). Immune checkpoint blockade (ICB) can control tumor growth and sometimes leads to regression of metastatic disease. ICB therapy targeting the inhibitory receptor PD1 (anti-PD1) is the most effective single-agent ICB treatment to date, while combination ICB targeting both PD1 and CTLA4 (anti-PD1/CTLA4) further increases response rates; however, with increased immune-related toxicity (4–7). In contrast to BRAF-directed targeted therapy (BRAFi; BRAF or combination BRAF/MEK inhibition), ICB therapies can induce durable long-term antitumor immune responses. These therapies have materially changed prognosis for patients with metastatic melanoma. Nevertheless, primary resistance to ICB is common, and one-third of ICB-treated patients with melanoma who have an initial response will subsequently progress (8). Furthermore, existing biomarkers to predict response to ICB therapy are controversial and limited by an incomplete understanding of the pretreatment immunologic features of the tumor microenvironment. Resistance to ICB can involve a number of factors or causes, including the upregulation of other inhibitory checkpoints (9, 10). As such, significant efforts are underway to understand which factors in the tumor microenvironment modify sensitivity to current ICB therapies to define alternative or ancillary immune checkpoint targets that improve outcomes and minimize toxicity.

A novel ICB target is the adhesion molecule CD155, which additionally functions as an immune checkpoint ligand expressed by tumor cells and tumor-associated myeloid cells (11). CD155 modifies lymphocyte function through multiple cognate immune receptors; TIGIT, CD96, and CD226 (DNAM-1), expressed by T and NK cells. CD155 is upregulated on tumor cells across multiple solid cancer types,

[1]Immunology in Cancer and Infection Laboratory, QIMR Berghofer Medical Research Institute, Queensland, Australia. [2]Cancer Immunoregulation and Immunotherapy Laboratory, QIMR Berghofer Medical Research Institute, Queenland, Australia. [3]School of Medicine, University of Queensland, Queensland, Australia. [4]Medical Genomics, QIMR Berghofer Medical Research Institute, Queensland, Australia. [5]Department of Medical Oncology, Cancer Care Services, Royal Brisbane and Women's Hospital, Brisbane, Australia. [6]Department of Melanoma, Cancer Immunotherapy and Development Therapeutics, Instituto Nazionale Tumori IRCCS Fondazione Pascale, Napoli, Italy. [7]Department of Surgery and Translational Medicine, University of Florence, Florence, Italy. [8]Department of Oncology and Haematology, Papa Giovanni XXIII Hospital, Bergamo, Italy. [9]Melanoma Institute Australia, The University of Sydney, New South Wales, Australia. [10]Department of Pathology, University of Montreal Health Center, Montreal, Quebec, Canada. [11]Research Centre, University of Montreal Hospital, Montreal, Canada. [12]Sydney Medical School, The University of Sydney, Sydney, New South Wales, Australia. [13]Department of Tissue Pathology and Diagnostic Oncology, Royal Prince Alfred Hospital and NSW Health Pathology, Sydney, New South Wales, Australia. [14]Oncology and Cellular Immunology, QIMR Berghofer Medical Research Institute, Herston, Queensland, Australia.

Note: Supplementary data for this article are available at Clinical Cancer Research Online (http://clincancerres.aacrjournals.org/).

A. Lepletier and J. Madore contributed equally to this article.

Corresponding Author: Mark J. Smyth, QIMR Berghofer Medical Research Institute, 300 Herston Road, Herston, Queensland 4006, Australia. Phone: 617-3845-3957; Fax: 617-3362-0111; E-mail: mark.smyth@qimr.edu.au

Clin Cancer Res 2020;XX:XX–XX

doi: 10.1158/1078-0432.CCR-19-3925

Published OnlineFirst April 28, 2020; DOI: 10.1158/1078-0432.CCR-19-3925

Translational Relevance

This is the first study to demonstrate that high tumor CD155 expression affects response to anti-PD1 therapy in patients with metastatic melanoma. CD155 promotes anti-PD1 resistance and increased PD1 expression on $CD8^+$ T cells within melanoma tumor parenchyma.

including melanoma, and has been shown to be advantageous to tumor growth and tumor survival (12). Recently, using mouse tumor models in which CD155 was knocked-out ($CD155^{KO}$), we demonstrated that loss of tumor CD155 increased sensitivity to combination anti-PD1/CTLA4 treatment *in vivo* (11), suggesting that cotargeting CD155 may complement current ICB therapies. It is unclear in humans to what extent tumor CD155 impacts the immune infiltrate contexture or whether expression of CD155 in human cancers affects sensitivity to immunotherapies. In this study, we characterize CD155 expression in human metastatic melanoma and provide evidence for a significant correlation between high CD155 and decreased sensitivity to ICB therapies. In PDL1 negative tumors, high tumor CD155 identified those patients who did not respond to combination anti-PD1/anti-CTLA4 therapy. We demonstrated that tumor CD155 correlated with an increase in the ratio of $PD1^+CD8^+$ T cells infiltrating melanoma tumor parenchyma, but not among T cells localized within the tumor stroma. Furthermore, a high intratumor $PD1^+CD8^+/CD8^+$ T-cell ratio ($PD1^{tR}$) was a predictor of poor response to PD1-based ICB therapy.

Results

High tumor CD155 limits response of patients with metastatic melanoma to αPD1-combitherapy

Following from our preclinical studies using mouse tumor models (11), we wanted to understand the impact of CD155 in human cancer. We characterized tumor CD155 protein levels using IHC in pretreatment surgical specimens from patients with metastatic melanoma who were treated with ICB [either anti-PD1 alone (αPD1-monotherapy) or in combination with anti-CTLA4 (αPD1-combitherapy)] or BRAFi therapy (**Fig. 1A**). In pretreatment tumor specimens ($n = 155$, ICB-treated; $n = 50$, BRAFi therapy), intratumor membrane staining for CD155 was highly constitutive/homogeneous. This is in contrast to the high intratumor heterogeneity and low-level expression observed for PDL1 in metastatic melanomas (13). However, considerable variation in the level of intrapatient CD155 membrane staining intensity was observed. Briefly, 5% (10/205) of melanoma pretreatment specimens were negative for CD155 (score 0+), 22% (45/205) were classified as membrane score 1+, 37% (75/205) were score 2+, and 37% (75/205) were score 3+ (**Table 1**). CD155 score 3+ tumors were characterized by strong circumferential membrane staining. Overall, this indicates that expression of CD155 by tumor cells is common in metastatic melanoma (>95%) but that significant interpatient variability exists at the level of CD155 membrane expression.

To appreciate whether tumor CD155 might influence response to ICB, we compared RECIST response categories (14) with pretreatment CD155 H-scores from patients treated with either αPD1-combitherapy or αPD1-monotherapy. We found that αPD1-combitherapy patients whose pretreatment tumors were CD155 score 3+ ($CD155^{high}$) demonstrated higher rates of stable disease (SD) or progressive disease (PD) as their best ICB response, and lower rates of complete response (CR) or partial response (PR), compared with patients who had CD155 low tumors [score 0+, 1+, 2+ ($CD155^{low}$); $P = 0.042$, FEPT (**Fig. 1B**)]. Furthermore, a significant association between disease progression within 6 months of ICB commencement and high CD155 tumor levels in αPD1-combitherapy–treated patients with melanoma was observed ($P = 0.007$, FEPT; **Fig. 1C**). Interestingly, in patients with melanoma treated with BRAFi therapy, $CD155^{high}$ tumors had a better RECIST response profile ($P = 0.002$, FEPT; **Fig. 1B**), but not better or worse PFS (**Fig. 1C**).

Associations between CD155 and therapy response were further evaluated using PFS and Kaplan-Meier and Cox proportional hazard modeling. For patients with melanoma treated with αPD1-combitherapy, median PFS was shorter in those patients with $CD155^{high}$ tumors compared with $CD155^{low}$ tumors [HR = 2.886 (1.11–7.504); $P = 0.007$; **Fig. 1D**]. For αPD1-monotherapy–treated patients, a similar trend in PFS was observed but it did not reach statistical significance (**Fig. 1D**). For patients treated with BRAFi therapy, no difference in PFS by CD155 tumor expression levels was observed (**Fig. 1D**) even though $CD155^{high}$ tumors responded better to BRAFi therapy by RECIST criteria (**Fig. 1B**). A comparison of PFS between αPD1-monotherapy and αPD1-combitherapy demonstrated improved outcome in $CD155^{low}$ tumors treated with αPD1-combitherapy [HR = 2.0 (1.1–3.8); $P = 0.032$], but no significant benefit was seen in $CD155^{high}$ patients by the addition of anti-CTLA4 therapy [HR = 1.0 (0.5–2.1); $P = 0.933$; Supplementary Fig. S1A].

$CD155^{high}$/PDL1 negative melanomas respond poorly to anti-PD1 therapy and show decreased expression of critical genes involved in T-cell function

We next compared tumor CD155 with immunotherapy outcome for PDL1 negative and PDL1 positive melanomas. Patients whose tumors were PDL1 negative and $CD155^{high}$ had poor RECIST response (no PR or CR in this group; **Fig. 2A**), regardless of whether they received αPD1-combitherapy ($P = 0.0009$) or αPD1-monotherapy ($P = 0.05$). Patients treated with αPD1-combitherapy whose tumors were PDL1 negative and $CD155^{high}$ also had worse 6-month PFS rates ($P = 0.05$; **Fig. 2B**), and shorter median PFS [HR = 6.12 (1.3–29.8); $P < 0.0001$; **Fig. 2C**]. In contrast, patients with PDL1 negative tumors whose CD155 expression was low had better PFS outcome, similar to those patients whose tumors were PDL1 positive.

We next wanted to understand how the level of CD155 protein expressed by tumor cells affected the immune cell contexture in human tumors. Gene expression data generated from pretreatment tumor specimens from 41 patients with metastatic melanoma were analyzed and compared with CD155 scores from surgically matched archival-FFPE tumor specimens. Using principal component analysis, no association between PC1 or PC2 and CD155 IHC score was determined, suggesting that CD155 was not associated with features underlying the basic biology of these tumors (Supplementary Fig. S1B). CD155 score by IHC correlated significantly with *PVR* (*CD155*) gene expression ($R = 0.604$; $P < 0.001$; Supplementary Fig. S1C). Next, we determined differentially expressed (DE) genes between CD155 score 1+ versus score 3+ tumors to represent low and high levels of CD155 protein expression ($n = 867$ genes, $P < 0.01$; Supplementary Table S1). Reactome pathway analyses were used to identify significantly enriched biological processes. Pathways significantly downregulated in CD155 score 3+ tumors included IFNγ signaling among other T cell–related pathways (**Fig. 2D**; Supplementary Fig. S1D), which suggested an association between CD155 and reduced $CD8^+$ T-cell function. Genes in the IFN signaling pathway DE

Published OnlineFirst April 28, 2020; DOI: 10.1158/1078-0432.CCR-19-3925

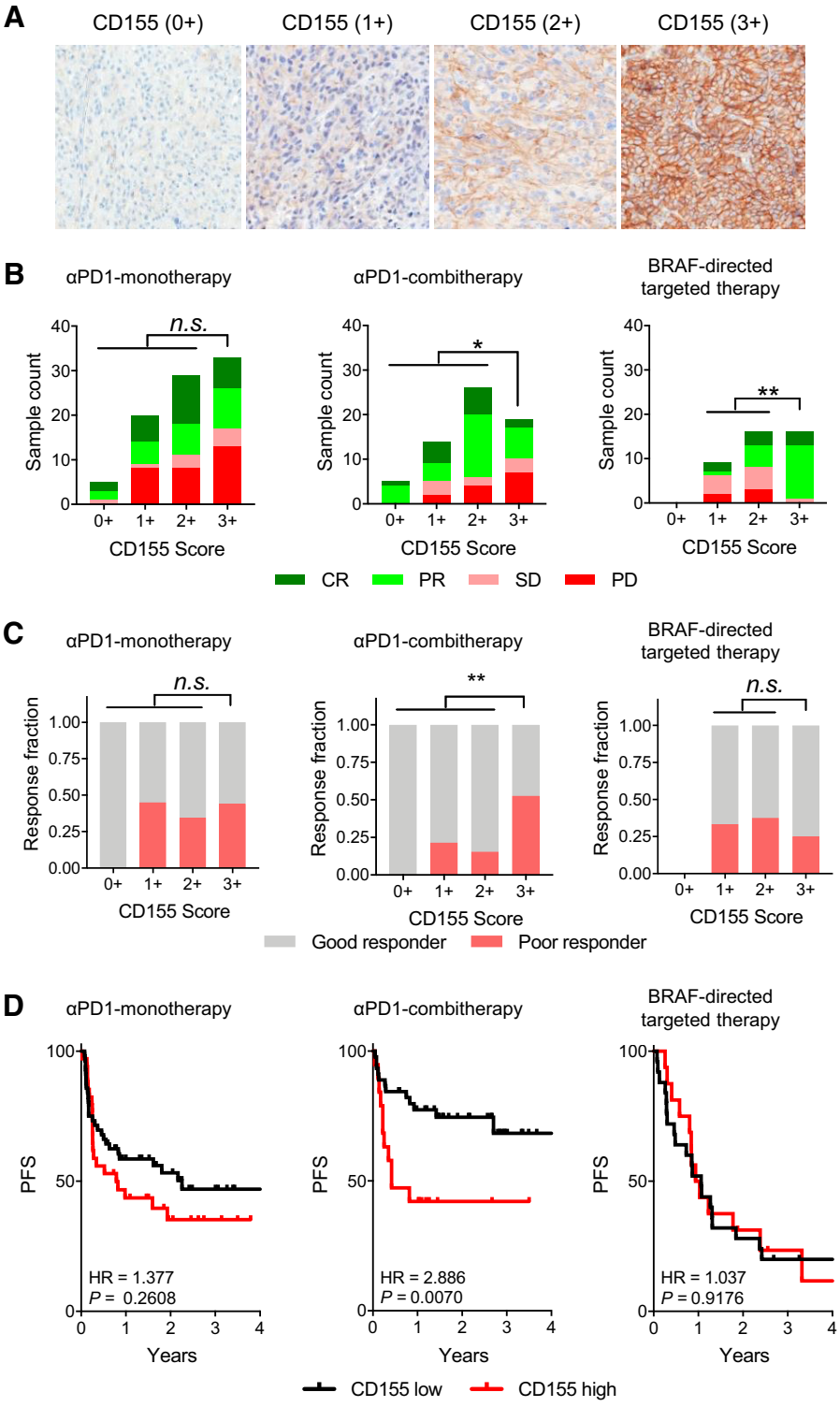

Figure 1.

High tumor CD155 expression limits response of patients with metastatic melanoma to αPD1-combitherapy and predicts better RECIST response to BRAFi-targeted therapy. **A,** Representative IHC images of CD155 H-scores (0+, 1+, 2+, 3+) from metastatic melanoma tumor specimens. **B,** Histograms for CD155 H-scores by RECIST category (CR, PR, SD, PD) in pretreatment tumor specimens from patients with metastatic melanoma treated with either αPD1-combitherapy (n = 64 patients), αPD1-monotherapy (n = 87 patients), or BRAFi therapy (n = 41 patients). FEPT by CR+PR versus SD+PD and $CD155^{low}$ (score 0+, 1+, 2+) versus $CD155^{high}$ (score 3+; *, $P < 0.05$; **, $P < 0.01$; n.s., not significant). **C,** The fraction of patients with progression-free response to therapy > 6 months. FEPT by response > 6 months and response < 6 months versus $CD155^{low}$ (score 0+, 1+, 2+) versus $CD155^{high}$ (score 3+; **, $P < 0.01$; n.s., not significant). **D,** Association of pretreatment tumor CD155 H-scores, $CD155^{low}$ (0+,1+,2+) versus $CD155^{high}$ (3+) with PFS evaluated using the Kaplan–Meier method and Cox proportional hazard modeling in patients with melanoma treated with αPD1-monotherapy (n = 57, $CD155^{low}$; n = 34, $CD155^{high}$; HR = 1.377; P = 0.26), αPD1-combitherapy (n = 45, $CD155^{low}$; n = 19, $CD155^{high}$; HR = 2.886; P = 0.007), or BRAFi therapy (n = 25, $CD155^{low}$; n = 16, $CD155^{high}$; HR = 1.037; P = 0.9176).

between CD155 score 1+ versus 3+ are shown in the heatmap clustered by CD155 score and PDL1 status (**Fig. 2E**). Out of 52 DE genes, 51 were downregulated in $CD155^{high}$ tumors. Among score 3+ tumors, there were outlier patients who had a PFS response > 6 months and these tumors were often PDL1 positive and showed higher expression of IFN-related genes. Together, these data suggest that CD155 plays a critical role in promoting tumor immune suppression in the context of anti-PD1 therapy, but this suppression might be overcome by a robust preexisting pretreatment immune response.

Published OnlineFirst April 28, 2020; DOI: 10.1158/1078-0432.CCR-19-3925

Table 1. Specimen cohort details.

	(MIA) melanoma	(RBWH) melanoma	(INT-IRCCS) melanoma	(PG-XXIII) melanoma
Specimen details				
n	101	33	21	50
Sex				
Female	24	8	9	23
Male	62	25	12	27
Unknown	15			
Median age (start of IO)	67	68	64	54
Surgery type				
Excision	101	25	21	50
Biopsy		8		
Multiplex-IF data	Yes	Yes	No	Yes
Tissue microarray	Yes	Yes	No	Yes
Therapy details				
Nivolumab	16		7	
Pembrolizumab	33	29	3	
Ipilimumab + Nivolumab	18	4	8	
Ipilimumab + Pembrolizumab	34		3	
1st line BRAFi targeted therapy	7	6	2	41
Clinically reported variables				
BRAF mutant	22	7	6	50
BRAF wild type	60	26	15	
LDH elevated	16		10	
LDH normal	63		10	
RECIST category/RECIST response				
PD	22	10	10	9
PR	42	6	3	16
SD	6	4	7	8
CR	28	11	1	8
No data	3	2		
Progression summary				
# censored subjects	64	16	3	8
# events (progression)	37	17	18	33
Median PFS (years)	4.83	0.82	0.42	1.03
Median follow-up	1.38	0.63	0.41	1.56
Survival summary				
# censored subjects	75	19	5	10
# events (death)	26	14	16	31
Median OS (years)	Undefined	Undefined	0.833	1.85
Median follow-up	1.68	1.44	0.82	2.14
CD155 H-Score				
0+ (0)	7	0	3	0
1+ (1–99)	23	7	4	11
2+ (100–199)	35	14	9	17
3+ (200–300)	36	12	5	22

Tumor CD155 correlates with increased PD1 expression on tumor-infiltrating CD8$^+$ T cells

RNA-seq analysis of pretreatment melanoma specimens suggested that tumor CD155 might influence the phenotype and function of tumor-infiltrating CD8$^+$ T cells. Here, we used multiplex-immunohistofluorescence (multiplex-IF) to examine the expression of the key inhibitory receptor PD1 on CD8$^+$ T cells (**Fig. 3A**). Melanoma tissue arrays or whole slide tissue sections from archival specimens were used and multiplex-IF data were matched to CD155 H-scores. Samples were enriched for high lymphocyte content selected by a pathologist using morphologically stained (H&E) slides. Tumor parenchyma (SOX10$^+$) and stromal regions (SOX10$^-$) were separately analyzed (**Fig. 3B**). Parenchymal CD8$^+$ T-cell counts did not correlate with tumor CD155 score indicating that T-cell infiltration is independent of tumor CD155 score (**Fig. 3C**). In contrast, the number of parenchymal PD1$^+$CD8$^+$ T cells significantly correlated with increasing CD155 score ($R = 0.248$; $P = 0.015$; **Fig. 3C**). Notably, the ratio of parenchymal PD1$^+$CD8$^+$ T cells to total CD8$^+$ T cells (PD1^{tR}) significantly correlated with tumor CD155 score ($R = 0.359$; $P = 0.0001$; **Fig. 3C**). These correlations were validated in an independent cohort of pretreatment melanoma specimens from patients who received targeted therapy only (**Fig. 3D**). Interestingly, no correlation was found for the same ratio calculated for stromal-localized PD1$^+$CD8$^+$ T cells (data not shown). In summary, our data support the notion that tumor CD155 protein expression is associated with increased PD1 expression on tumor-infiltrating CD8$^+$ T cells specifically within a PD1^{high} CD8$^+$ T-cell phenotype, but does not affect the recruitment of T cells into the melanoma parenchyma.

Published OnlineFirst April 28, 2020; DOI: 10.1158/1078-0432.CCR-19-3925

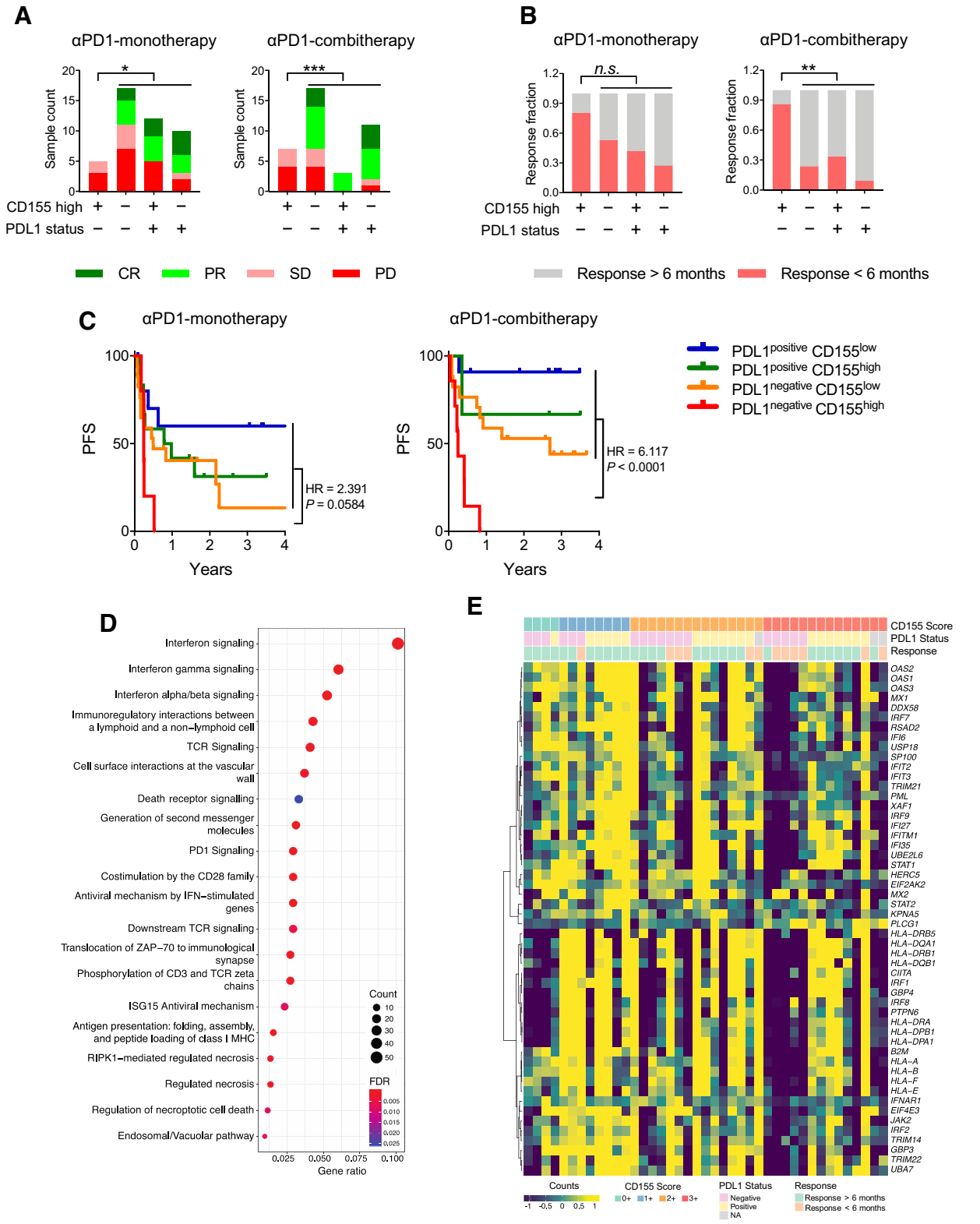

Figure 2.

Anti-PD1 therapy is ineffective in PDL1 negative melanomas that are high for CD155 expression and CD155 high tumors show decreased expression of critical genes involved in T-cell function. **A,** Bar plots of RECIST response categories (CR, PR, SD, PD) in metastatic melanoma by PDL1 status and CD155 tumor expression [$CD155^{high}$ (3+] vs. $CD155^{low}$ (0+, 1+, 2+)] in pretreatment tumor specimens from patients with metastatic melanoma treated with either αPD1-combitherapy ($n = 38$ patients) or αPD1-monotherapy ($n = 44$ patients). (*Continued on the following page.*)

Published OnlineFirst April 28, 2020; DOI: 10.1158/1078-0432.CCR-19-3925

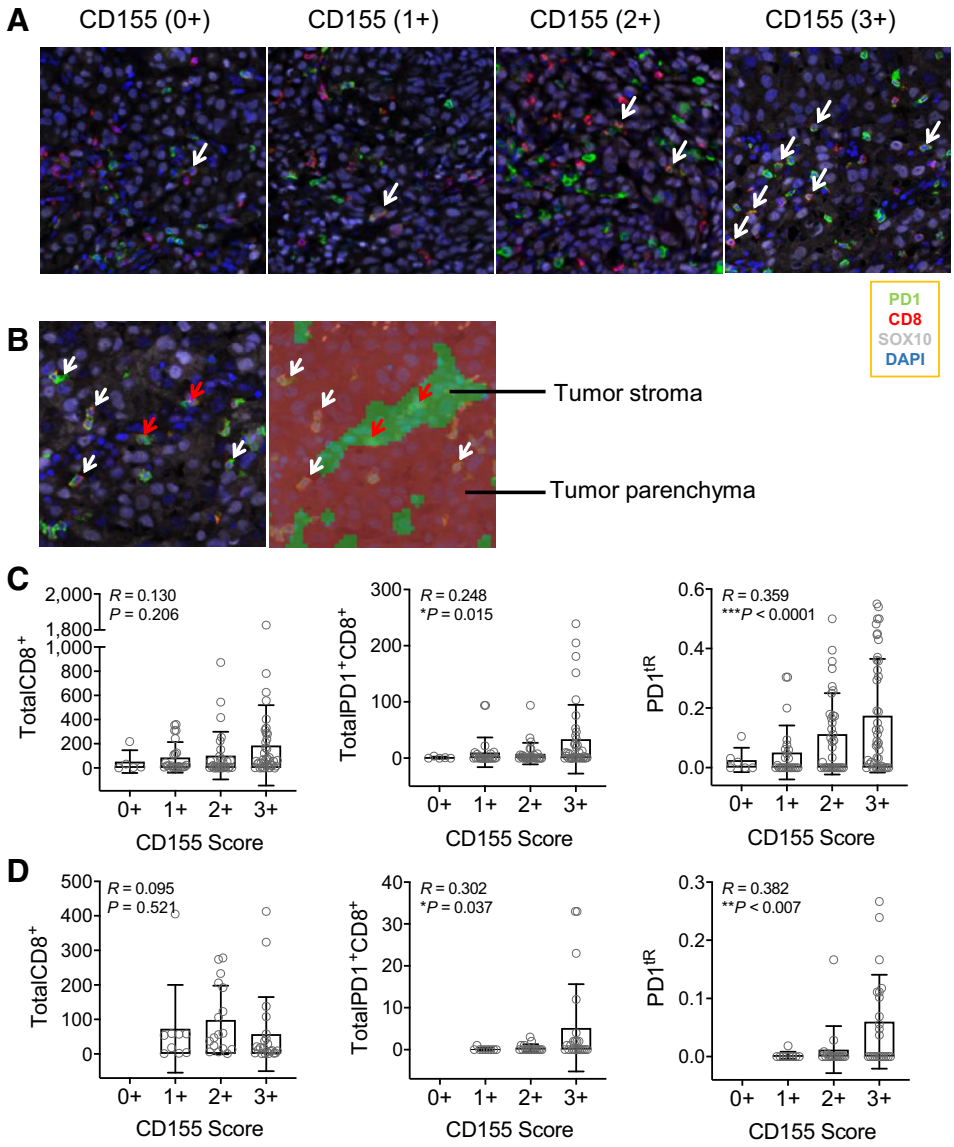

Figure 3.

Intratumor ratio of PD1^{+}CD8^{+} T cells to total CD8^{+} T cells correlates with tumor CD155 levels. **A,** Representative multiplex-IF composite images of melanoma tumors with increasing CD155 score stained for CD8^{+} (red), PD1^{+} (green), and SOX10^{+} (light gray nuclei). White arrows indicate PD1^{+}CD8^{+} lymphocytes. **B,** Representative images for computational image analysis defining tissue category regions showing tumor parenchyma and tumor stroma with CD8^{+} T cells in tumor stroma indicated by red arrows and CD8^{+} T cells in tumor parenchyma indicated by white arrows. **C,** Data summaries of total counts for tumor-infiltrating CD8^{+} lymphocytes ($R = 0.130$; $P = 0.206$), total PD1^{+}CD8^{+} lymphocytes ($R = 0.248$; $P = 0.015$), and the ratio of PD1^{+}CD8^{+} to total CD8^{+} lymphocytes (PD1^{tR}; $R = 0.359$; $P < 0.0001$), against CD155 H-score in pretreatment specimens from immunotherapy-treated patients with metastatic melanoma ($n = 106$ patients). **D,** Validation of data in (**C**) using an independent cohort of patients treated with BRAFi therapy ($n = 48$ patients). Data summaries of total counts for tumor-infiltrating CD8^{+} lymphocytes ($R = 0.095$; $P = 0.521$), total PD1^{+}CD8^{+} lymphocytes ($R = 0.302$; $P = 0.037$), and PD1^{tR} ($R = 0.382$; $P < 0.007$). Pearson correlation coefficient analyses were used (**C** and **D**) to assess the relationship between CD155 H-score and CD8^{+} T cells, PD1^{+}CD8^{+} T cells, and PD1^{tR}. Exact P values and R coefficients have been included in each chart.

Increased PD1^{tR} is associated with PD and early disease progression

We evaluated the impact of high PD1^{tR} on RECIST categories and PFS outcome. Compared with CD155 score, a high PD1^{tR} was more significantly associated with poor RECIST categories and with higher rates of PD and SD in patients with αPD1-combitherapy– and αPD1-monotherapy–treated melanoma ($P = 0.001$ and 0.007 respectively, FEPT; **Fig. 4A**). A significant association between disease progression within 6 months of ICB commencement and high PD1^{tR} in patients with αPD1-combitherapy– and αPD1-monotherapy–treated melanoma was observed ($P = 0.008$ and 0.007 respectively, FEPT; **Fig. 4B**). Shorter PFS correlated with high PD1^{tR} in patients with αPD1-combitherapy–treated melanoma [HR = 7.301 (1.808–29.49); $P = 0.0032$] and in αPD1-monotherapy–treated patients [HR = 1.905 (0.7571–4.793); $P = 0.094$; **Fig. 4C**]. We next compared the predictive value of PD1^{tR} with therapy-specific outcome. As expected, αPD1-combitherapy resulted in better PFS for patients with melanoma with low PD1^{tR}, compared with αPD1-monotherapy [HR = 5.658 (2.431–13.17); $P = 0.007$;

(*Continued.*) FEPT by CR+PR versus SD+PD and PDL1^{negative}/CD155^{high} versus other scores. *, $P < 0.05$; ***, $P < 0.001$. **B,** The fraction of patients with response > 6 months by PDL1 status and CD155 tumor expression. FEPT by response > 6 months versus response < 6 months and PDL1^{negative}/CD155^{high} versus other scores. **, $P < 0.01$; n.s., not significant. **C,** PFS of patients with metastatic melanoma categorized by PDL1 status and CD155 tumor expression. Association between PDL1^{negative}/CD155^{high} versus other scores evaluated using Kaplan–Meier method. Patients were treated with either αPD1-monotherapy ($n = 11$, CD155^{low}/PDL1^{positive}; $n = 12$, CD155^{high}/PDL1^{positive}; $n = 5$, CD155^{high}/PDL1^{negative}; $n = 17$, CD155^{low}/PDL1^{negative}; HR = 2.391; $P = 0.0584$) or αPD1-combitherapy ($n = 11$, CD155^{low}/PDL1^{positive}; $n = 3$, CD155^{high}/PDL1^{positive}; $n = 7$, CD155^{high}/PDL1^{negative}; $n = 17$, CD155^{low}/PDL1^{negative}; HR = 6.117; $P < 0.0001$). **D,** The top 20 enriched Reactome pathways from differential gene expression analysis ($P < 0.01$) of CD155 H-score 1+ versus 3+ melanomas. **E,** Heatmap of genes that contribute to the Reactome pathway "Interferon signaling" (R-HSA-913531). Patients are clustered according to CD155 H-score (from left to right: 0+, 1+, 2+, 3+) followed by PDL1 status ($n = 41$ patients).

Published OnlineFirst April 28, 2020; DOI: 10.1158/1078-0432.CCR-19-3925

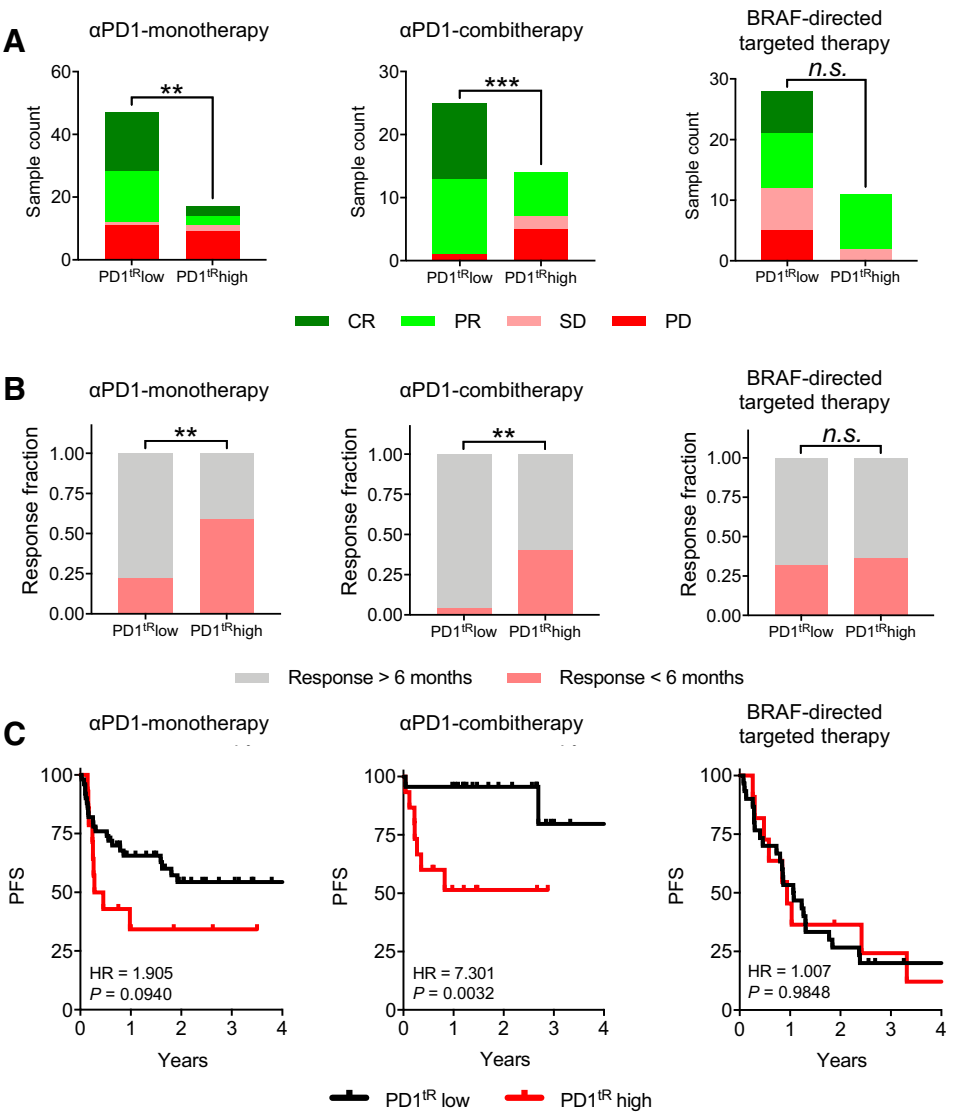

Figure 4.

PD1^{tR} correlates with response to immunotherapy but not targeted therapy treated metastatic melanoma. **A,** Histogram of immunotherapy RECIST response categories (CR, PR, SD, PD) from αPD1-combitherapy (n = 39), αPD1-monotherapy (n = 64), and BRAFi therapy (n = 39) treated patients with metastatic melanoma. FEPT by CR+PR versus SD+PD and PD1^{tR}low versus PD1^{tR}high. **, $P < 0.01$; ***, $P < 0.001$; n.s., not significant. **B,** The fraction of patients with therapy response >6 months by PD1^{tR} measured in pretreatment tumor specimens. FEPT by response > 6 months versus response < 6 months and PD1^{tR}low versus PD1^{tR}high. **, $P < 0.01$; n.s., not significant. **C,** Association of pretreatment tumor PD1^{tR} with PFS evaluated using the Kaplan–Meier method and Cox proportional hazard modeling in αPD1-combitherapy (n = 39; HR = 7.301; P = 0.0032), αPD1-monotherapy (n = 66; HR = 1.905; P = 0.094), and BRAFi therapy (n = 41; HR = 1.007; P = 0.9848), treated patients with metastatic melanoma.

Supplementary Fig. S1A]. However, for patients with melanoma with high PD1^{tR}, αPD1-combination therapy did not lead to improved PFS over that seen for patients treated with αPD1-monotherapy [HR = 1.582 (0.6108–4.1); P = 0.345; Supplementary Fig. S1A]. We additionally wanted to understand whether the effect of PD1^{tR} on outcome was specific to immunotherapy-treated patients. In *BRAF*-mutated patients with melanoma who did not receive anti-PD1 therapy, but received BRAFi therapy, there was no association between RECIST response or PFS outcome with PD1^{tR} (**Fig. 4C**).

Discussion

Development of alternative checkpoint therapies to compliment or substitute anti-PD1 and anti-CTLA4 are the subject of intensive academic and industrial pharmaceutical studies. In this study, we found that in metastatic melanoma, pretreatment CD155 tumor levels affected response to αPD1-combination therapy suggesting that targeting the CD155 pathway might be beneficial in patients with anti-PD1 refractory melanoma. A possible mechanism underpinning this observation is tumor CD155 signaling through the immune checkpoint receptors CD96 and TIGIT to promote CD8$^+$ T-cell inhibition. Elevated CD155 tumor expression was found to correlate with an increase in the ratio of PD1$^+$CD8$^+$ T cells within the tumor parenchyma (PD1^{tR}), and this increase was associated with PD and early time to progression among αPD1-combination–treated patients with melanoma. The detrimental effect of high CD155 expression was evident but was not statistically significant in αPD1-monotherapy–treated patients. One explanation for this might be the greater effectiveness of αPD1-combination therapy (15), resulting in more impressive RECIST response and survival outcomes for patients with favorable tumor CD155 expression. Furthermore, CD155 suppression of therapeutic response was specific to ICB-treated patients as it was not observed in patients with melanoma treated with BRAFi therapy, indicating that tumor CD155 specifically limits sensitivity to ICB therapy in metastatic melanoma. Indeed, in BRAFi-treated patients, a high tumor CD155 predicted better RECIST response albeit with no difference in PFS compared with patients whose tumors were CD155 low. Given these data, we hypothesize that cotargeting the CD155 pathway (CD96/TIGIT coblockade) in combination with anti-PD1 therapy

might increase response rates in patients with anti-PD1 refractory melanoma.

Analysis of the spatial distribution of lymphocyte subsets in tumors can be predictive and reveal aspects of tumor biology not apparent in gross T-cell estimations typically achieved in flow cytometry data (16–18). We found a positive correlation between CD155 tumor levels and $PD1^{tR}$ when lymphocytes were counted within the tumor parenchyma, but not for lymphocytes counted within the tumor stroma. This suggests that $PD1^{tR}$ might partially be driven by the interaction of the CD155 ligand on tumor cells with its cognate T-cell receptors (TIGIT and CD96). Furthermore, this parenchymal interaction of tumor CD155 and T cells could be affecting sensitivity to anti-PD1 therapy (11). Better PFS outcome was observed in $CD155^{high}$ tumors which had a favorable pretreatment PDL1 status and IFN gene signatures, reflecting an active pretreatment antitumor immune response (19–22). However, no apparent statistical benefit from combination therapy coupled with the inferior survival outcomes in patients with $CD155^{high}$ or high $PD1^{tR}$ tumors suggests that additional or alternative treatment approaches are required for those patients, possibly including blockade of CD155 interactions with TIGIT and CD96. The immunosuppressive effect of CD155 on response to anti-PD1 therapy was most apparent in PDL1 negative tumors that scored 3+ for CD155, regardless of ICB therapy type, and this group of patients showed no complete or partial RECIST responses.

Interestingly, CD155 negative tumors consistently demonstrated excellent outcome to ICB therapy; however, RNA-seq of CD155 negative melanoma tumors indicated a diminished IFN gene signature and were often PDL1 negative. This suggests that tumors of this type do not contain a pretreatment immune response and this is particularly interesting given that PDL1 negative tumors with limited IFN gene signatures are generally thought to respond poorly to immunotherapy (19–22). However, CD155 has an intrinsic role in mediating tumor cell growth and invasion and these tumors may represent a less aggressive melanoma tumor type (11). Nevertheless, given the positive response of CD155 negative tumors to ICB, the absence of an existing intratumor immune response before treatment must not preclude the development of one on treatment, at least not in CD155 negative melanomas. A caveat is that the natural history of CD155 negative tumors is unknown and this may be an intrinsically positive prognostic factor independent of ICB treatment. In any case, CD155 negative melanomas are rare (<5%) and the biology of CD155 negative tumors deserves greater scrutiny.

We have previously shown in mice that expression of CD155 in the tumor microenvironment limits the efficacy of tumor growth control by T and NK cells (11, 23, 24). Recently, it has been shown that $PD1^{hi}CD8^+$ T cells in chronic infection and cancer are dysfunctional and in fact epigenetically repressed and terminally differentiated, as such, this population is insensitive to anti-PD1 therapy (25, 26). Given that multiplex-IF is less sensitive than conventional flow cytometry, it may be reasonable to assume that $PD1^+CD8^+$ T cells as detected by multiplex-IF in patient samples are those expressing the highest levels of PD1 ($PD1^+CD8^+ = PD1^{hi}CD8^+$) and therefore likely to have a dysfunctional phenotype. While we have not demonstrated that the $PD1^+CD8^+$ T-cell population observed by multiplex IHC in pretreatment human melanoma specimens was dysfunctional *per se*, the combination of our observations made by IHC and bulk tumor RNA-seq supports a model in which tumor cell CD155 expression correlates with high $PD1^{tR}$ levels thought to be associated with a dysfunctional $CD8^+$ T-cell phenotype. Importantly, varied mechanisms of resistance to anti-PD1 therapy can affect response rates (9, 27–30). Nevertheless, CD155 is commonly expressed in metastatic melanoma lesions (>95%) indicating the CD155 pathway is an attractive immunotherapy cotarget in anti-PD1 ICB therapy.

$CD8^+$ T cells infiltrating human melanoma also express TIGIT and CD96 in addition to PD1 (24, 31, 32). Therefore, it may be reasonable to propose that the inhibitory signaling mediated not only through PD1, but also CD96 and TIGIT, drives T-cell dysfunction. Indeed, coblockade of PD1 and CD96 in established CT26 colon adenocarcinomas increased IFNγ production above that observed for anti-PD1 blockade, suggesting that these cell populations may be amenable to functional reinvigoration (23). Furthermore, therapeutic blockade of TIGIT and CD96 had superior activity in controlling primary tumor growth compared with αPD1-monotherapy in B16F10 melanoma tumor models (23). In mouse tumor models using CD155-deficient mice, it was previously shown that both tumor and host CD155 were critical for tumor growth, so therapeutic targeting of TIGIT and CD96 must take this into consideration (11). The contribution of CD155-dependent signaling could potentially be assessed in early-phase clinical trials of anti-TIGIT as monotherapy or in combination with anti-PD1 (NCT02964013), and in other future randomized controlled trials targeting members of this pathway.

In summary, we have shown that high expression of CD155 in metastatic melanoma correlates with an increase in the intratumor ratio of $PD1^+CD8^+/CD8^+$ T cells, abbreviated here as $PD1^{tR}$, and reduced sensitivity to αPD1-combitherapy. It is likely that $PD1^+CD8^+$ T cells detected by multiplex-IF are of a $PD1^{hi}$ phenotype and thus dysfunctional and resistant to PD1-based ICB reinvigoration. Furthermore, CD155 combined with PDL1 might be a useful predictor of a group of patients who do not respond to anti-PD1 ICB. Our findings give impetus for validation in a prospective cohort the utility of CD155 plus PDL1 as a predictive biomarker, and for clinical trials to assess therapies blocking CD96/TIGIT or CD155 in combination with anti-PD1 therapy.

Materials and Methods

Patients and specimens

The study was approved by the QIMR Berghofer Human Research Ethics Committee (HREC). Research involving human subjects was also approved by HRECs at each clinical site and was conducted according to the Declaration of Helsinki. Where prospective biospecimen collection was undertaken, informed consent was granted by study participants. For retrospective annotated specimens, a waiver of consent was gained by the site HREC. Retrospective archival-FFPE (formalin-fixed, paraffin-embedded) tissue specimens were obtained for patients with radiologically confirmed stage IV melanoma (American Joint Committee on Cancer) from four institutional sites: Melanoma Institute Australia (MIA), Royal Brisbane Women's Hospital (RBWH), Istituto Nazionale Tumori - IRCCS (INT-IRCCS), and Papa Giovanna XXIII Hospital (PG-XXIII). Presence of tumor cells was monitored by hematoxylin and eosin (H&E) staining. Patient demographics, primary tumor characteristics, and therapy details are listed in Table 1. Fresh tumor specimens for RNA sequencing (RNA-seq) analysis were collected through the MIA tumor biobank. REMARK guidelines (33) were followed where data were available from the contributing institute.

IHC

Archival-FFPE tumors were sectioned at 3 μm on superfrost+ slides. Slides were dehydrated at 65°C for 20 minutes, deparaffinized in xylene, and rehydrated in graded ethanol. Antigen retrieval was performed in Tris/Ethylenediaminetetraacetic acid (EDTA) buffer

Published OnlineFirst April 28, 2020; DOI: 10.1158/1078-0432.CCR-19-3925

(Agilent Technologies; S236784-2) (pH 9) in a Decloaking Chamber (Biocare Medical) at 100°C for 20 minutes. IHC was performed on an Autostainer-Plus (DAKO). Primary antibodies against CD155 (D3G7H; Cell Signaling Technology, catalog no. 13544) or PDL1 (E1L3N; Cell Signaling Technology, catalog no. 13684) were incubated for 45 minutes at room temperature using a 1:100 dilution for CD155 or 1:150 for PDL1. Staining was visualized using a Rabbit-HRP-polymer detection system (Biocare; M3R531) and DAB Chromogen Kit (Biocare; BDB2004) and counterstained with diluted hematoxylin. IHC was evaluated for two representative high-power fields of view noting the percentage of membrane positive tumor cells and the maximum intensity of IHC signal (0+ to 3+). CD155 score was assigned using the blinded H-score method and categorized as follows; score 0+ (negative), score 1+ (0–99), score 2+ (100–199), or score 3+ (200–300). PDL1 score was assigned as the combined percentage of PDL1 positive tumor and inflammatory cells per representative whole specimen slide.

Multiplex immunohistofluorescence

Archival-FFPE tissue specimens were sectioned at 3 μm onto Superfrost+ slides. Slides were then deparaffinized, rehydrated, and washed in tris-buffered saline with 0.01% Tween-20 (TBS-T). Antigen retrieval was performed in modified citrate buffer pH 6.1 (Agilent Technologies; S169984-2) at 100°C for 20 minutes. All multiplex steps were performed using an Autostainer Plus (DAKO, Agilent Technologies) with two TBS-T washes between each step. Tissue sections were blocked with 3% hydrogen peroxide in TBS-T for 5 minutes and background sniper for 10 minutes (Biocare Medical). Sequential staining was performed using the Opal method (PerkinElmer) with antibody stripping steps performed in Tris/EDTA buffer (Agilent Technologies; S236784-2) at 100°C for 20 minutes. Primary antibodies incubated for 30 minutes, followed by two-step polymer-HRP detection (Biocare; Mach3) and then labeled with tyramide signal amplification–based fluorophores (PerkinElmer; Opal Reagent Pack). The following primary antibodies/clones were used sequentially in the order listed; PD1/NAT105 (1:500;Opal520), CD8/144b (1:7,500; Opal570), and SOX10/BC34 (1:600; Opal690). Slides were counterstained with DAPI and coverslipped (DAKO; S3023).

Multiplex-IF image acquisition and analysis

Images were obtained using the Vectra 3.0 slide scanner (PerkinElmer) under the appropriate fluorescent filters. A fluorescent whole slide scan at 4× magnification was produced and visualized in Phenochart (v1.0.4), followed by multispectral image acquisition of each tissue microarray core or selected high power regions at 20× magnification. Multispectral images were spectrally unmixed followed by tissue and cell segmentation using InForm analysis software (v2.2.1). Nuclear expression of SOX10 by tumor cells was used to segment melanoma tumor parenchyma and stroma tissue regions. Merged data files from InForm were preprocessed and fluorescence thresholds were set using Spotfire image-mapping tools for each marker ($PD1^+$, $CD8^+$, and $SOX10^+$; Tibco Spotfire Analyst, v7.6.1) followed by segmented cell counting using Spotfire and tabulation in Microsoft Excel.

RNA-seq preparation, data processing, and differential expression analysis

RNA-seq was performed on pretreatment tumor specimens from 41 patients with metastatic melanoma treated with immunotherapy at Melanoma Institute Australia (NSW, Australia). Briefly, total RNA was isolated from fresh frozen tissue sections using the AllPrepDNA/RNA/miRNA Universal Kit (Qiagen) according to the manufacturer's instructions (34, 35). RNA quantity was assessed on Qubit, and RNA integrity was assessed using the RNA 6000 Nano kit and run on the Agilent 2100 Bioanalyzer (Agilent Technologies). cDNA synthesis and library construction were performed using the TruSeq RNA Library Prep Kit (Illumina) and paired-end 100 bp sequencing, with each sample yielding 40–50 million reads. Sequencing was performed on the Illumina Hiseq 2500 platforms at the Australian Genome Research Facility in Melbourne. Fastq data were downloaded and sequence reads were trimmed for adapter sequences using Cutadapt (version 1.9; ref. 36) and aligned using STAR (version 2.5.2A) to the GRCh37 human reference genome assembly using the gene, transcript, and exon features model of Ensembl (release 70). Quality control metrics were computed using RNA-SeQC (version 1.1.8) and transcript abundances were quantified using RSEM (version 1.2.30). Further analysis of the RNA-seq data was carried out in R (version 3.5.1). Protein-coding genes with < 3 counts per million in fewer than 5 samples were removed from downstream analyses. Trimmed mean of M-values (TMM) normalization and differential gene expression analysis were performed using the edgeR package (37). The "prcomp" function in R was used to perform principal component analysis on genewise centered and scaled values of TMM normalized expression data. To perform pathway analysis, the "clusterProfiler::bitr" function (38) was used to convert gene IDs from Ensembl to Entrez, then consequently passed to the "ReactomePA::enrichPathway" function (39), before plotting the results with the "clusterProfiler::dotplot" function (38). Heatmaps were produced using "ComplexHeatmap" R package (40, 41) using genwise centered, scaled, $\log_2$ values of TMM normalized expression data, and "Pearson" distance with "ward.D" criteria to cluster the rows. RNA-seq data analyzed in this study have been published (42) and deposited in the European Genome-phenome Archive (EGA) under dataset accession EGAD00001005501 and study accession EGAS00001001552.

Outcome analysis

Univariate survival analysis was carried out by fitting Cox proportional hazard models to dichotomize patient groups according to respective variables and the survival variable. Cut-off points for the dichotomized variable were calculated as the arithmetic mean of the two successive values which gave the most significant logrank split using cut-off finder version 2.0 (43). HRs including 95% confidence intervals are calculated and log-rank *P* values given. Progression-free survival (PFS) was defined as time from commencement of therapy to documented disease progression (PFS). Response to ICB was assessed by site investigators using timepoint RECIST version 1.1 (i.e., best response in time-point fashion).

Statistical methods and data availability

Correlations between categorical clinical variables and experimental variables (CD155, $PD1^{tR}$) were calculated using a two-tailed Fisher exact probability test (FEPT). Correlations of CD155 IHC with immune cell counts by multiplex-IF were performed using Pearson *R* method. Statistical analyses listed in figure legends were performed using PRISM. All data for multiplex-IF and chromogenic IHC supporting the findings of this study are available from the corresponding author upon reasonable request. RNA-seq data have been deposited in the European Genome-Phenome Archive (accession number: EGAD00001005501).

Published OnlineFirst April 28, 2020; DOI: 10.1158/1078-0432.CCR-19-3925

Disclosure of Potential Conflicts of Interest

M. Eastgate is an advisory board member/unpaid consultant for and reports receiving other remuneration from Novartis. P.A. Ascierto reports receiving commercial research grants from Bristol-Myers Squibb, Roche-Genentech, and Array, is an advisory board member/unpaid consultant for Bristol-Myers Squibb, Roche-Genentech, MSD, Array, Novartis, Merck Serono, Pierre Fabre, Incyte, New Link Genetics, Genmab, Medimmune, AstraZeneca, Syndax, SunPharma, Sanofi, Idera, UltimoVacs, Sandoz, Immunocore, 4SC, Alkermes, Italfarmaco, Nektar, and Boehringer-Ingelheim, and other remuneration from MSD. M. Mandala reports receiving speakers bureau honoraria from Bristol-Myers Squibb, MSD, Novartis, and Pierre Fabre. A.M. Menzies is an employee/paid consultant for Bristol-Myers Squibb, MSD, Novartis, Roche, and Pierre Fabre. J. Stagg is an employee/paid consultant for, reports receiving other commercial research support from, and holds ownership interest (including patents) in Surface Oncology. G.V. Long is an advisory board member/unpaid consultant for Aduro, Amgen, Bristol-Myers Squibb, Mass-Array, Merck, MSD, Novartis, OncoSec Medical, Pierre Fabre, Roche, and Sandoz. R.A. Scolyer is an employee/paid consultant for Royal Prince Alfred Hospital, MSD, GlaxoSmithKline Australia, Bristol-Myers Squibb, Novartis Pharmaceuticals Australia Pty Ltd, Myriad, NeraCare, and Amgen, and reports receiving commercial research grants from NHMRC. T. Bald is an employee/paid consultant for Oncomyx and reports receiving commercial research grants from ENA therapeutics and Bristol-Myers Squibb. N. Waddell holds ownership interest (including patents) in genomiQa. W.C. Dougall is an employee/paid consultant for Cascadia Drug Development Group, QIMR Berghofer Medical Research Inst., and Omeros Corp., reports receiving commercial research grants from Bristol-Myers Squibb, and speakers bureau honoraria from Amgen. M.J. Smyth is an employee/paid consultant for Tizona Therapeutics and Compass Therapeutics, and reports receiving commercial research grants from Bristol-Myers Squibb, Tizona Therapeutics, and Aduro Biotech. No potential conflicts of interest were disclosed by the other authors.

Authors' Contributions

Conception and design: A. Lepletier, J. Madore, J.S. O'Donnell, J.S. Wilmott, T. Bald, W.C. Dougall, M.J. Smyth

Development of methodology: A. Lepletier, J. Madore, R.L. Johnston, X.-Y. Li, D. Mallardo

Acquisition of data (provided animals, acquired and managed patients, provided facilities, etc.): J. Madore, E. McDonald, E. Ahern, A. Kuchel, M. Eastgate, S.-A. Pearson, D. Mallardo, P.A. Ascierto, D. Massi, B. Merelli, M. Mandala, J.S. Wilmott, A.M. Menzies, C. Leduc, J. Stagg, G.V. Long, R.A. Scolyer

Analysis and interpretation of data (e.g., statistical analysis, biostatistics, computational analysis): A. Lepletier, J. Madore, J.S. O'Donnell, R.L. Johnston, E. Ahern, A. Kuchel, P.A. Ascierto, J.S. Wilmott, C. Leduc, R.A. Scolyer, T. Bald, N. Waddell

Writing, review, and/or revision of the manuscript: A. Lepletier, J. Madore, J.S. O'Donnell, E. Ahern, A. Kuchel, P.A. Ascierto, D. Massi, M. Mandala, J.S. Wilmott, A.M. Menzies, B. Routy, G.V. Long, R.A. Scolyer, T. Bald, W.C. Dougall, M.W.L. Teng, M.J. Smyth

Administrative, technical, or material support (i.e., reporting or organizing data, constructing databases): J. Madore, S.-A. Pearson, J.S. Wilmott, M.J. Smyth

Study supervision: J. Madore, M. Mandala, N. Waddell, W.C. Dougall, M.J. Smyth

Other (provided human bio specimen samples): G.V. Long

Acknowledgments

A. Lepletier, J. Madore, and W.C. Dougall. and some of the work were supported by a scientific research agreement from Bristol Myers Squibb and a project grant from the Australian Skin and Skin Cancer Research Centre. S.-A. Pearson was supported by philanthropic funding from Terry Jackman. T. Bald was supported by a National Health and Medical Research Council (NH&MRC) Early Career Research Fellowship (1138757). M.W.L. Teng was supported by a NH&MRC Career Development Fellowship (1159655) and Project Grant (1120887). M.J. Smyth was supported by a NH&MRC Senior Principal Research Fellowship (1078671), a NH&MRC Program Grant (1132519) and a CCQ Project Grant (1157048). For R.A. Scolyer, some of this work was supported by a NHMRC Program Grant (G.V. Long and R.A. Scolyer) and the NHMRC Fellowship program (J.S. Wilmott, G.V. Long, and R.A. Scolyer). Funding support from Melanoma Institute Australia (MIA) and The Ainsworth Foundation is also gratefully acknowledged. The authors also thank colleagues at Royal Prince Alfred Hospital and MIA for assistance.

We thank the patients who participated in this study; clinical faculty and personnel, including Bianca Nowlan for technical assistance; Gunter Hartel for statistical support, the histology and microscopy department at QIMR Berghofer, staff and clinicians at Melanoma Institute Australia; Helen Rizos and Richard Kefford for providing tumor specimens. The authors also thank Robert Johnston, Bristol Myers Squibb, for very helpful discussion.

The costs of publication of this article were defrayed in part by the payment of page charges. This article must therefore be hereby marked *advertisement* in accordance with 18 U.S.C. Section 1734 solely to indicate this fact.

Received December 2, 2019; revised March 30, 2020; accepted April 24, 2020; published first April 28, 2020.

References

1. Chen DS, Mellman I. Oncology meets immunology: the cancer-immunity cycle. Immunity 2013;39:1–10.
2. O'Donnell JS, Teng MWL, Smyth MJ. Cancer immunoediting and resistance to T cell-based immunotherapy. Nat Rev Clin Oncol 2019;16:151–67.
3. Thommen DS, Schumacher TN. T cell dysfunction in cancer. Cancer Cell 2018; 33:547–62.
4. Hellmann MD, Ciuleanu T-E, Pluzanski A, Lee JS, Otterson GA, Audigier-Valette C, et al. Nivolumab plus ipilimumab in lung cancer with a high tumor mutational burden. N Engl J Med 2018;378:2093–104.
5. Larkin J, Chiarion-Sileni V, Gonzalez R, Grob JJ, Cowey CL, Lao CD, et al. Combined nivolumab and ipilimumab or monotherapy in untreated melanoma. N Engl J Med 2015;373:23–34.
6. Long GV, Larkin J, Ascierto PA, Hodi FS, Rutkowski P, Sileni V, et al. PD-L1 expression as a biomarker for nivolumab (NIVO) plus ipilimumab (IPI) and NIVO alone in advanced melanoma (MEL): a pooled analysis. Ann Oncol 2016; 27(suppl_6).
7. Wei SC, Duffy CR, Allison JP. Fundamental mechanisms of immune checkpoint blockade therapy. Cancer Discov 2018;8:1069–86.
8. Schachter J, Ribas A, Long GV, Arance A, Grob J-J, Mortier L, et al. Pembrolizumab versus ipilimumab for advanced melanoma: final overall survival results of a multicentre, randomised, open-label phase 3 study (KEYNOTE-006). Lancet 2017;390:1853–62.
9. Gide TN, Quek C, Menzies AM, Tasker AT, Shang P, Holst J, et al. Distinct immune cell populations define response to anti-PD-1 monotherapy and anti-PD-1/anti-CTLA-4 combined therapy. Cancer Cell 2019;35:238–55.e6.
10. Fares CM, Van Allen EM, Drake CG, Allison JP, Hu-Lieskovan S. Mechanisms of resistance to immune checkpoint blockade: why does checkpoint inhibitor immunotherapy not work for all patients? Am Soc Clin Oncol Educ Book 2019;39:147–64.
11. Li XY, Das I, Lepletier A, Addala V, Bald T, Stannard K, et al. CD155 loss enhances tumor suppression via combined host and tumor-intrinsic mechanisms. J Clin Invest 2018;128:2613–25.
12. Bevelacqua V, Bevelacqua Y, Candido S, Skarmoutsou E, Amoroso A, Guarneri C, et al. Nectin like-5 overexpression correlates with the malignant phenotype in cutaneous melanoma. Oncotarget 2012;3:882–92.
13. Madore J, Vilain RE, Menzies AM, Kakavand H, Wilmott JS, Hyman J, et al. PD-L1 expression in melanoma shows marked heterogeneity within and between patients: implications for anti-PD-1/PD-L1 clinical trials. Pigment Cell Melanoma Res 2015;28:245–53.
14. Schwartz LH, Litiere S, de Vries E, Ford R, Gwyther S, Mandrekar S, et al. RECIST 1.1-update and clarification: from the RECIST committee. Eur J Cancer 2016;62: 132–7.
15. Wolchok JD, Chiarion-Sileni V, Gonzalez R, Rutkowski P, Grob JJ, Cowey CL, et al. Overall survival with combined nivolumab and ipilimumab in advanced melanoma. N Engl J Med 2017;377:1345–56.
16. Nguyen N, Bellile E, Thomas D, McHugh J, Rozek L, Virani S, et al. Tumor infiltrating lymphocytes and survival in patients with head and neck squamous cell carcinoma. Head Neck 2016;38:1074–84.
17. Oguejiofor K, Hall J, Slater C, Betts G, Hall G, Slevin N, et al. Stromal infiltration of CD8 T cells is associated with improved clinical outcome in HPV-positive oropharyngeal squamous carcinoma. Br J Cancer 2015;113:886–93.

18. Shimizu S, Hiratsuka H, Koike K, Tsuchihashi K, Sonoda T, Ogi K, et al. Tumor-infiltrating CD8 T-cell density is an independent prognostic marker for oral squamous cell carcinoma. Cancer Med 2019;8:80–93.
19. Ayers M, Lunceford J, Nebozhyn M, Murphy E, Loboda A, Kaufman DR, et al. IFN-γ-related mRNA profile predicts clinical response to PD-1 blockade. J Clin Invest 2017;127:2930–40.
20. Hugo W, Zaretsky JM, Sun L, Song C, Moreno BH, Hu-Lieskovan S, et al. Genomic and transcriptomic features of response to anti-PD-1 therapy in metastatic melanoma. Cell 2017;168:542.
21. Bald T, Landsberg J, Lopez-Ramos D, Renn M, Glodde N, Jansen P, et al. Immune cell-poor melanomas benefit from PD-1 blockade after targeted type I IFN activation. Cancer Discov 2014;4:674–87.
22. Gajewski TF, Corrales L, Williams J, Horton B, Sivan A, Spranger S. Cancer immunotherapy targets based on understanding the T cell-inflamed versus non-T cell-inflamed tumor microenvironment. Adv Exp Med Biol 2017;1036:19–31.
23. Blake SJ, Stannard K, Liu J, Allen S, Yong MCR, Mittal D, et al. Suppression of metastases using a new lymphocyte checkpoint target for cancer immunotherapy. Cancer Discov 2016;6:446–59.
24. Mittal D, Lepletier A, Madore J, Aguilera AR, Stannard K, Blake SJ, et al. CD96 is an immune checkpoint that regulates CD8 T-cell antitumor function. Cancer Immunol Res 2019;97:152–64.
25. Ngiow SF, Young A, Jacquelot N, Yamazaki T, Enot D, Zitvogel L, et al. A threshold level of intratumor CD8+ T-cell PD1 expression dictates therapeutic response to anti-PD1. Cancer Res 2015;75:3800–11.
26. Sen DR, Kaminski J, Barnitz RA, Kurachi M, Gerdemann U, Yates KB, et al. The epigenetic landscape of T cell exhaustion. Science 2016;354:1165–9.
27. Smyth MJ, Ngiow SF, Ribas A, Teng MW. Combination cancer immunotherapies tailored to the tumour microenvironment. Nat Rev Clin Oncol 2016;13:143–58.
28. Spranger S, Bao R, Gajewski TF. Melanoma-intrinsic beta-catenin signalling prevents anti-tumour immunity. Nature 2015;523:231–5.
29. Neubert NJ, Schmittnaegel M, Bordry N, Nassiri S, Wald N, Martignier C, et al. T cell-induced CSF1 promotes melanoma resistance to PD1 blockade. Sci Transl Med 2018;10.
30. Gao J, Shi LZ, Zhao H, Chen J, Xiong L, He Q, et al. Loss of IFN-gamma pathway genes in tumor cells as a mechanism of resistance to anti-CTLA-4 therapy. Cell 2016;167:397–404.e9.
31. Chauvin JM, Pagliano O, Fourcade J, Sun Z, Wang H, Sander C, et al. TIGIT and PD-1 impair tumor antigen-specific CD8(+) T cells in melanoma patients. J Clin Invest 2015;125:2046–58.
32. Lepletier A, Lutzky VP, Mittal D, Stannard K, Watkins TS, Ratnatunga CN, et al. The immune checkpoint CD96 defines a distinct lymphocyte phenotype and is highly expressed on tumor-infiltrating T cells. Immunol Cell Biol 2019;97:152–64.
33. McShane LM, Altman DG, Sauerbrei W, Taube SE, Gion M, Clark GM. REporting recommendations for tumour MARKer prognostic studies (REMARK). Br J Cancer 2005;93:387–91.
34. Hayward NK, Wilmott JS, Waddell N, Johansson PA, Field MA, Nones K, et al. Whole-genome landscapes of major melanoma subtypes. Nature 2017;545:175–80.
35. Wilmott JS, Hayward NK, Mann GJ, Scolyer RA. Advantages of whole-genome sequencing for identification of tumor etiology and clinically actionable genomic aberrations: lessons from the Australian melanoma genome project. Melanoma Manag 2017;4:147–9.
36. Martin M. Cutadapt removes adapter sequences from high-throughput sequencing reads. EMBnet.journal 2011;17:10–2.
37. Robinson MD, McCarthy DJ, Smyth GK. edgeR: a Bioconductor package for differential expression analysis of digital gene expression data. Bioinformatics 2010;26:139–40.
38. Yu G, Wang LG, Han Y, He QY. clusterProfiler: an R package for comparing biological themes among gene clusters. OMICS 2012;16:284–7.
39. Yu G, He QY. ReactomePA: an R/Bioconductor package for reactome pathway analysis and visualization. Mol Biosyst 2016;12:477–9.
40. Rooney MS, Shukla SA, Wu CJ, Getz G, Hacohen N. Molecular and genetic properties of tumors associated with local immune cytolytic activity. Cell 2015;160:48–61.
41. Gu Z, Eils R, Schlesner M. Complex heatmaps reveal patterns and correlations in multidimensional genomic data. Bioinformatics 2016;32:2847–9.
42. Lee J SE, Shklovskaya E, Lim SY, Carlino M. Menzies A, Stewart A, et al. Transcriptional downregulation of MHC class I and melanoma de-differentiation in resistance to PD-1 inhibition. Nat Commun 2020;11:1897.
43. Budczies J, Klauschen F, Sinn BV, Győrffy B, Schmitt WD, Darb-Esfahani S, et al. Cutoff finder: a comprehensive and straightforward web application enabling rapid biomarker cutoff optimization. PLoS One 2012;7:e51862.

Published OnlineFirst April 28, 2020; DOI: 10.1158/1078-0432.CCR-19-3925

Clinical Cancer Research

Tumor CD155 Expression Is Associated with Resistance to Anti-PD1 Immunotherapy in Metastatic Melanoma

Ailin Lepletier, Jason Madore, Jake S. O'Donnell, et al.

Clin Cancer Res Published OnlineFirst April 28, 2020.